Gomez *et al. Mol Brain* (2021) 14:20
https://doi.org/10.1186/s13041-020-00714-1

Molecular Brain

RESEARCH Open Access

Non-SUMOylated CRMP2 decreases $Na_V1.7$ currents via the endocytic proteins Numb, Nedd4-2 and Eps15

Kimberly Gomez[1†], Dongzhi Ran[1†], Cynthia L. Madura[1], Aubin Moutal[1] and Rajesh Khanna[1,2*]

Abstract

Voltage-gated sodium channels are key players in neuronal excitability and pain signaling. Functional expression of the voltage-gated sodium channel $Na_V1.7$ is under the control of SUMOylated collapsin response mediator protein 2 (CRMP2). When not SUMOylated, CRMP2 forms a complex with the endocytic proteins Numb, the epidermal growth factor receptor pathway substrate 15 (Eps15), and the E3 ubiquitin ligase Nedd4-2 to promote clathrin-mediated endocytosis of $Na_V1.7$. We recently reported that CRMP2 SUMO-null knock-in ($CRMP2^{K374A/K374A}$) female mice have reduced $Na_V1.7$ membrane localization and currents in their sensory neurons. Preventing CRMP2 SUMOylation was sufficient to reverse mechanical allodynia in $CRMP2^{K374A/K374A}$ female mice with neuropathic pain. Here we report that inhibiting clathrin assembly in nerve-injured male $CRMP2^{K374A/K374A}$ mice precipitated mechanical allodynia in mice otherwise resistant to developing persistent pain. Furthermore, Numb, Nedd4-2 and Eps15 expression was not modified in basal conditions in the dorsal root ganglia (DRG) of male and female $CRMP2^{K374A/K374A}$ mice. Finally, silencing these proteins in DRG neurons from female $CRMP2^{K374A/K374A}$ mice, restored the loss of sodium currents. Our study shows that the endocytic complex composed of Numb, Nedd4-2 and Eps15, is necessary for non-SUMOylated CRMP2-mediated internalization of sodium channels in vivo.

Keywords: CRMP2, Sumoylation, Endocytosis, $Na_V1.7$, Numb, Eps15, Nedd4-2, Neuropathic pain

Introduction

$Na_V1.7$ is a voltage-gated sodium channel highly expressed in nociceptive neurons and in the dorsal horn of the spinal cord [1]. Biophysically, $Na_V1.7$ manifests as a fast-activating and inactivating channel with slow repriming (recovery from inactivation) kinetics, with sensitivity to tetrodotoxin (TTX-S) [2]. $Na_V1.7$ acts as a threshold channel to propagate action potentials in response to depolarizations of sensory neurons by noxious stimuli [3]. Past research has established $Na_V1.7$ as both necessary and sufficient for pain sensitivity [4, 5]. Also well documented is the role of $Na_V1.7$ during neuropathic and inflammatory pain, wherein $Na_V1.7$ channel function and membrane expression are increased, resulting in hyperexcitability of dorsal root ganglia (DRG) neurons, likely via an amplification of subthreshold depolarizations [6].

Studies over the last decade in our laboratory have identified the collapsin response mediator protein 2 (CRMP2) as a regulator of diverse receptors [7–9], exchangers [10, 11], and ion channels [12–23], including $Na_V1.7$ [24–26]. Regulation of $Na_V1.7$ function follows CRMP2′s post-translational modification states, primarily phosphorylation and SUMOylation (i.e. addition of a small ubiquitin like modifier (SUMO)). In rodent models mimicking chronic neuropathic pain

*Correspondence: rkhanna@arizona.edu
†Kimberly Gomez and Dongzhi Ran contributed equally to this work
[1] Department of Pharmacology, College of Medicine, University of Arizona, 1501 North Campbell Drive, P.O. Box 245050, Tucson, AZ 85724, USA
Full list of author information is available at the end of the article

© The Author(s) 2021. **Open Access** This article is licensed under a Creative Commons Attribution 4.0 International License, which permits use, sharing, adaptation, distribution and reproduction in any medium or format, as long as you give appropriate credit to the original author(s) and the source, provide a link to the Creative Commons licence, and indicate if changes were made. The images or other third party material in this article are included in the article's Creative Commons licence, unless indicated otherwise in a credit line to the material. If material is not included in the article's Creative Commons licence and your intended use is not permitted by statutory regulation or exceeds the permitted use, you will need to obtain permission directly from the copyright holder. To view a copy of this licence, visit http://creativecommons.org/licenses/by/4.0/. The Creative Commons Public Domain Dedication waiver (http://creativecommons.org/publicdomain/zero/1.0/) applies to the data made available in this article, unless otherwise stated in a credit line to the data.

states, CRMP2 phosphorylation by cyclin-dependent kinase 5 (Cdk5) at Ser522 (S522) is increased [27–30]; this is accompanied by enhanced SUMOylation by the E2-conjugating enzyme (Ubc9) at Lys374 (K374) [25, 31]. Increased CRMP2 SUMOylation facilitates $Na_V1.7$ membrane expression and increases the excitability of DRG neurons, and together these events may contribute to the expression of neuropathic pain [25, 26]. Loss of CRMP2 SUMOylation results in: (i) reduced $Na_V1.7$–CRMP2 binding; (ii) increased $Na_V1.7$ internalization via association and recruitment of a tripartite complex of proteins containing the endocytic protein Numb, the E3 ubiquitin ligase, the neuronal precursor cell expressed developmentally downregulated-4 type 2 (Nedd4-2), and epidermal growth factor receptor pathway substrate 15 (Eps15); and (iii) decreased $Na_V1.7$ surface expression and currents [25]. This reduction can be rescued by blocking clathrin mediated endocytosis or by deleting the endocytic proteins Numb, Nedd4-2 or Eps15 [25]. Numb is an endocytic adaptor protein that has been reported to bind to components of clathrin mediated endocytosis machinery [32]. Numb can recruit Nedd4-2 to mark $Na_V1.7$ for endocytosis by monoubiquitination [25, 33]. Eps15 then binds to the monoubiquitinated channel to induce the initial curvature of the membrane and allow for the clathrin coated pit to form [34, 35].

To determine the role of CRMP2 SUMOylation in vivo, we generated CRMP2 K374A knock-in ($CRMP2^{K374A/K374A}$) transgenic mice, in which the sole SUMOylation site on CRMP2 at Lysine 374 was replaced by an alanine [36]. Although CRMP2 SUMOylation was abolished in both male and female homozygous mice, we unexpectedly discovered that CRMP2 dependent $Na_V1.7$ trafficking was sexually dimorphic [37]. In female mice only, germline loss of CRMP2 SUMOylation reduced $Na_V1.7$–CRMP2 binding, $Na_V1.7$ membrane localization and $Na_V1.7$ currents in DRG sensory neurons, compared to their wildtype (WT) littermates [37]. Inhibiting clathrin assembly with Pitstop2 [38], rescued the decreased sodium currents back to the levels observed in DRG from WT female mice. In contrast, none of these effects were observed in male mice, suggesting that the $CRMP2^{K374A/K374A}$ mutation imposed a sex-specific regulation on $Na_V1.7$. Of relevance to the role of $Na_V1.7$ in pain, we found that $CRMP2^{K374A/K374A}$ mice of both sexes failed to develop mechanical allodynia after a spinal nerve injury (SNI) [37], thus supporting the conclusion that CRMP2 SUMOylation-dependent regulation of $Na_V1.7$ still holds in chronic neuropathic pain in male mice. Together, these studies underscore the critical role of CRMP2 SUMOylation as a regulatory mechanism underlying $Na_V1.7$ functional expression.

In this study, we asked two questions. First, is the lack of mechanical allodynia in male $CRMP2^{K374A/K374A}$ mice due to increased internalization of $Na_V1.7$? And second, is the decrease in $Na_V1.7$ currents in female $CRMP2^{K374A/K374A}$ mice reliant on the endocytic proteins Numb, Nedd4-2 and Eps15? Here, using $CRMP2^{K374A/K374A}$ mice, we show that: (i) inhibition of clathrin-mediated endocytosis restores nociception following SNI in male mice; (ii) Numb, Nedd4-2 and Eps15 expression is not different between DRGs from male and female mice; and (iii) knocking down these endocytic proteins in DRG neurons restores the loss of sodium currents observed in female $CRMP2^{K374A/K374A}$ mice. Together, our data resolve the mechanism of decreased $Na_V1.7$ membrane localization, currents and lack of allodynia in male and female $CRMP2^{K374A/K374A}$ mice.

Results

In vivo inhibition of clathrin assembly restores mechanical allodynia in male $CRMP2^{K374A/K374A}$ mice with spinal nerve injury.

Our previous in vitro studies found that the $CRMP2^{K374A/K374A}$ genotype leads to a reduction of sodium currents in female, but not male, mice [37]. Inhibiting clathrin assembly with the small molecule Pitstop2 [25], rescued the decrease in sodium currents observed in DRG neurons from female $CRMP2^{K374A/K374A}$ mice [37]. Subsequent in vivo studies revealed that, following SNI, both $CRMP2^{K374A/K374A}$ male and female mice become resistant to the development of mechanical allodynia compared to their WT littermates [37]. From these data, one can surmise that although there is no impact of loss of CRMP2 SUMOylation on sodium currents in male mice, inflicting a neuropathic pain injury uncovers an effect in both sexes [37]. To resolve this discrepancy, we hypothesized that increased internalization of $Na_V1.7$ in male $CRMP2^{K374A/K374A}$ mice compromises its role in neuropathic pain. As inhibiting clathrin assembly normalized $Na_V1.7$ current loss in female $CRMP2^{K374A/K374A}$ mice, we asked if Pitstop2 could precipitate mechanical allodynia in male $CRMP2^{K374A/K374A}$ mice with neuropathic pain. In male $CRMP2^{K374A/K374A}$ mice, we found higher paw withdrawal thresholds at day 42 in mice subjected to SNI compared to their WT littermates (Fig. 1; raw quantified numerical data for this and all subsequent figures is shown in Additional file 1: Table S1). After intrathecal administration of 0.1% DMSO (vehicle), WT mice maintained a low paw withdrawal threshold, whilst $CRMP2^{K374A/K374A}$ mice showed a persistent resistance to mechanical allodynia (Fig. 1). In contrast, administration of 2 μg/5 μl of Pitstop2 significantly decreased the paw withdrawal thresholds in male $CRMP2^{K374A/K374A}$ mice 1 h following the injection and then gradually recovered.

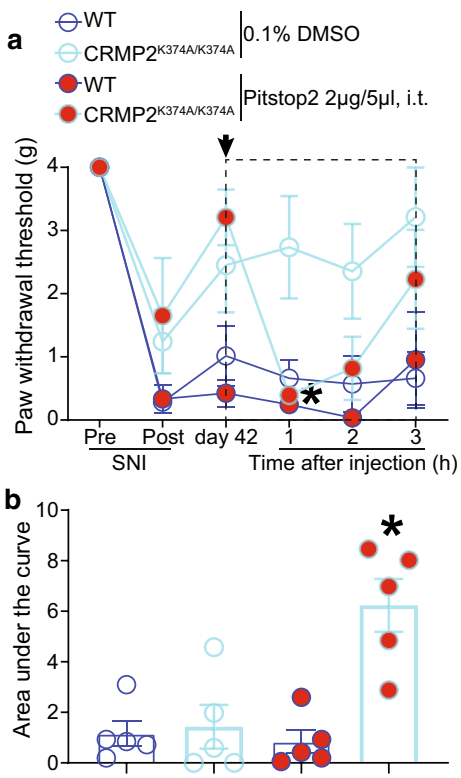

Fig. 1 Pitstop2 rescues mechanical allodynia in male CRMP2$^{K374A/K374A}$ knock-in mice with a spared nerve injury (SNI). Paw withdrawal thresholds of age-matched and genotyped WT and CRMP2$^{K374A/K374A}$ mice were measured at baseline and for six weeks following SNI. Post SNI, von Frey testing was confined to the sural nerve innervated region of the paw. **a** Time course showing that, at 42 days following SNI, male CRMP2$^{K374A/K374A}$ mice do not develop mechanical allodynia, which can however be precipitated by Pitstop2 administered by a lumbar puncture (2 μg in 5 μl) and followed over 3 h. *p < 0.05 two-way ANOVA with Sidak's post hoc test. **b** Area under the curve for paw withdrawal thresholds was derived using the trapezoid method and calculated from day 42 until 3 h after injection (dashed box in panel **a**). Error bars indicate mean ± SEM. *p < 0.05 Kruskal–Wallis test. The experiments were conducted by an investigator blinded to the genotype and treatment (n = 5 each)

No significant changes were observed in WT male mice (Fig. 1). Taken together, this data suggests that, in male CRMP2$^{K374A/K374A}$ mice, enhanced clathrin mediated endocytosis contributes to the resistance to mechanical allodynia in CRMP2$^{K374A/K374A}$ mice with SNI. This is consistent with our previous observations of increased CRMP2 SUMOylation in male rats with SNI [26].

Silencing Numb, Nedd4-2 and Eps15 rescues the decrement of sodium currents in female CRMP2$^{K374A/K374A}$ mice

Our previous study established that non-SUMOylated CRMP2 recruits Numb, Nedd4-2 and Eps15 to regulate internalization of $Na_V1.7$ channels [25]. In basal conditions, in male and female CRMP2$^{K374A/K374A}$ mice DRG, $Na_V1.7$ currents contribute to ~ 58% and ~ 76% of the total sodium currents, respectively [37]. However, Na^+ currents were decreased only in female CRMP2$^{K374A/K374A}$ mice while we could not measure any difference in their male littermates. We ruled out that the failure to observe this loss of $Na_V1.7$ currents in male CRMP2$^{K374A/K374A}$ DRGs was not due to lack of the neurotrophic factors nerve growth factor (NGF) or brain derived neurotrophic factor (BDNF) nor due to increased basal endocytic activity [37]. However, our previous work did not determine the level of expression of the endocytic proteins Numb, Nedd4-2 and Eps15. Consequently, here we asked if the levels of these proteins could explain the sex specific outcomes of CRMP2$^{K374A/K374A}$ mice. We dissected lumbar DRGs from male and female WT mice and detected the level of expression of Numb, Nedd4-2 and Eps15 by western blot. We did not find any significant difference of expression of these endocytic proteins between male and female animals (Fig. 2; raw data is shown in Additional file 2: Fig. S1). Hence, the sex difference in $Na_V1.7$ currents cannot not be attributed to changes in the expression of endocytic proteins that regulate its internalization.

Having demonstrated that inhibiting clathrin assembly in CRMP2$^{K374A/K374A}$ mice with neuropathic pain restores mechanical sensitivity, we next investigated the functional consequences of knocking-down each of the proteins that constitute the endocytic machinery. We used specific siRNAs (validated in [25]) to knockdown the expression of Numb (Fig. 3), Nedd4-2 (Fig. 4), or Eps15 (Fig. 5) in DRG neurons. Figures 3a, 4a and 5a display representative sodium currents recorded from female WT and CRMP2$^{K374A/K374A}$ DRG neurons transfected with siRNA control and siRNA against Numb (Fig. 3a), Nedd4-2 (Fig. 4a), or Eps15 (Fig. 5a). Silencing Numb, Nedd4-2 and Eps15 in CRMP2$^{K374A/K374A}$, restored the decreased sodium currents density (106.5%, 238.9% and 279.6%, respectively), back to the levels observed in DRG from CRMP2$^{K374A/K374A}$ transfected with a control siRNA (Fig. 3b, 4b and 5b). In contrast, silencing these proteins in DRG from WT mice had no effect (Fig. 3b, 4b and 5b). To account for the heterogeneity of the DRG population in terms of neuronal size, peaks were normalized by cell capacitance and subsequently displayed as peak current density (pA/pF). Again, there was restoration of peak currents in CRMP2$^{K374A/K374A}$ mice after knocking-down the endocytic proteins, while in WT mice there were no differences noted (Figs. 3c, 4c and 5c). To test if silencing Numb, Nedd4-2 and Eps15 could cause changes in channel gating, we next calculated the voltage-dependent activation and inactivation properties of sodium currents in

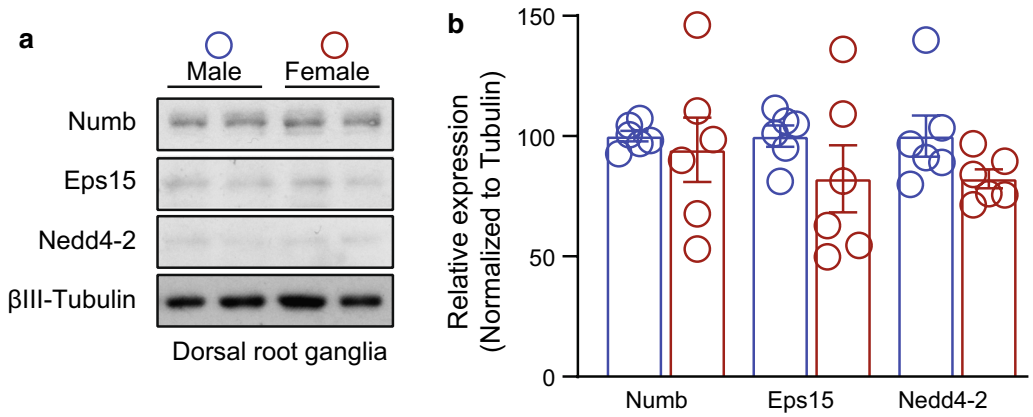

Fig. 2 Expression of Numb, Nedd4-2 and Eps15 in male and female mice DRGs. **a** Representative Western blots showing the expression of the endocytic proteins Numb, Nedd4-2 and Eps15 in lumbar DRG from male and female wildtype mice. βIII-tubulin served as a loading control. **b** Bar graph with scatter plot showing no difference of expression of the proteins between male and female DRG (n = 6)

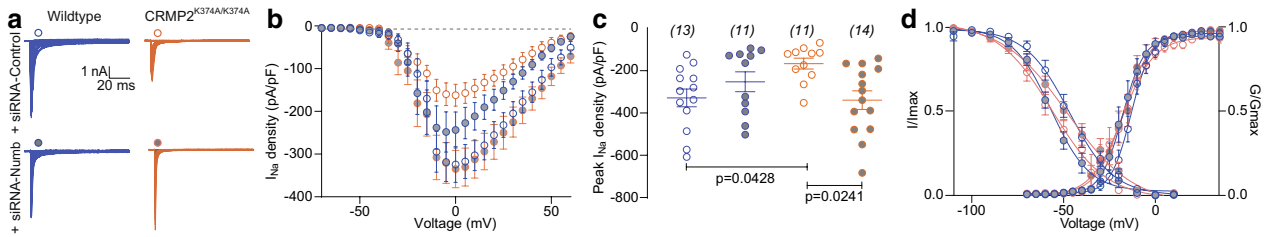

Fig. 3 CRMP2-mediated decrease in sodium currents observed in DRGs from CRMP2$^{K374A/K374A}$ mice is rescued in cells lacking Numb. **a** Representative sodium current traces recorded from small-sized DRG neurons of WT and CRMP2$^{K374A/K374A}$ female mice, in response to depolarization steps from − 70 to + 60 mV from a holding potential of − 60 mV. **b** Summary of current density–voltage curves and **c** peak current density (pA/pF) from DRG neurons. Total sodium current density was significantly smaller in DRGs from homozygous mice vs. DRG neurons from WT + siRNA-Control (n = 11 and 13 cells/condition, p = 0.0428, Kruskal–Wallis test with Dunn's post hoc), and vs. DRG neurons from CRMP2$^{K374A/K374A}$ + siRNA-Numb (n = 11 and 14, p = 0.0241, Kruskal–Wallis test with Dunn's post hoc). **d** Boltzmann fits for normalized conductance *G/Gmax*-voltage relations for voltage dependent activation and inactivation of the sensory neurons. Half-maximal activation and inactivation ($V_{1/2}$) and slope values (*k*) for activation and inactivation are presented in Table 1. There were no significant differences in $V_{1/2}$ and *k* values of activation and inactivation between genotype and treatment (One-way ANOVA with Dunnett's post hoc test). Error bars indicate mean ± SEM

DRG neurons. Comparing the midpoint potentials ($V_{1/2}$) and slope factors (*k*) in response to changes in command voltages (Table 1) of whole-cell ionic conductance, allowed us to measure changes in activation and inactivation of sodium currents for the DRG neurons transfected with siRNAs. Representative Boltzmann fits are shown in Figs. 3d, 4d and 5d. There were no significant differences in the steady-state activation and inactivation properties of sodium currents, per analysis of $V_{1/2}$ and *k* values, between DRG neurons of any condition (Table 1). Altogether, our results show that the lack of any of these endocytic proteins is sufficient to disrupt the endocytic complex to affect a rescue of the decreased sodium currents. This is entirely consistent with past results from rat DRG neurons overexpression of a sumo null CRMP2 [25].

Discussion

Our results provide further mechanistic insights into how loss of CRMP2 SUMOylation decreases $Na_v1.7$ currents in female mice and mechanical allodynia in male mice. We demonstrate that inhibiting clathrin assembly in male CRMP2$^{K374A/K374A}$ mice, following an injury that results in neuropathic pain, restores mechanical sensitivity. When determining the expression levels of the CRMP2 interacting endocytic proteins in the DRG, we found no differences between sexes under basal conditions. Furthermore, the reduction of Na^+ currents in DRG neurons from female CRMP2$^{K374A/K374A}$ mice were normalized by silencing Numb, Nedd4-2 and Eps15. The dynamic process of SUMOylation/deSUMOylation of CRMP2 controls the membrane surface expression and current density of $Na_V1.7$ channels in rodent and human DRGs

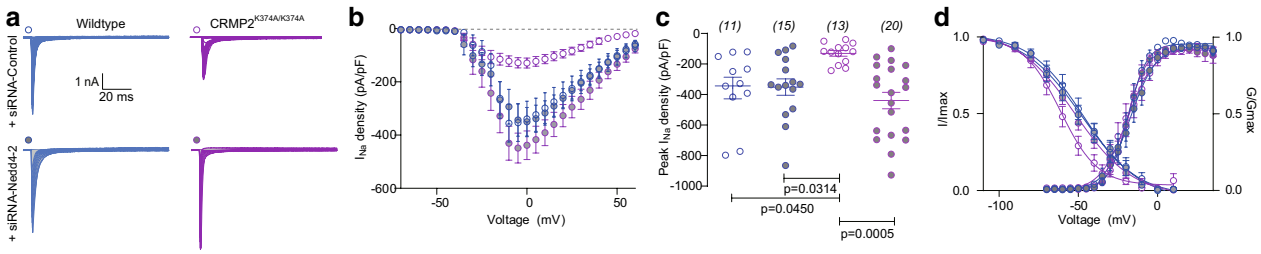

Fig. 4 CRMP2-mediated decrease in sodium currents observed in DRGs from CRMP2$^{K374A/K374A}$ mice is rescued in cells lacking Nedd4-2. **a** Representative sodium current traces recorded from small-sized DRG neurons of WT and CRMP2$^{K374A/K374A}$ female mice, in response to depolarization steps from − 70 to + 60 mV from a holding potential of − 60 mV. **b** Summary of current density–voltage curves and **c** peak current density (pA/pF) from DRG neurons. Total sodium current density was significantly smaller in DRGs from homozygous female mice vs. DRG neurons from WT + siRNA-Control (n = 13 and 11 cells/condition, p = 0.0450, Kruskal–Wallis test with Dunn's post hoc), vs. DRG neurons from WT + siRNA-Nedd4-2 (n = 13 and 15, p = 0.0314, Kruskal–Wallis test with Dunn's post hoc), and vs. DRG neurons from CRMP2$^{K374A/K374A}$ + siRNA-Nedd4-2 (n = 13 and 20, p = 0.0005, Kruskal–Wallis test with Dunn's post hoc). **d** Boltzmann fits for normalized conductance *G/Gmax*-voltage relations for voltage dependent activation and inactivation of the sensory neurons. Half-maximal activation and inactivation ($V_{1/2}$) and slope values (*k*) for activation and inactivation are presented in Table 1. There were no significant differences in $V_{1/2}$ and *k* values of activation and inactivation between genotype and treatment (One-way ANOVA with Dunnett's post hoc test). Error bars indicate mean ± SEM

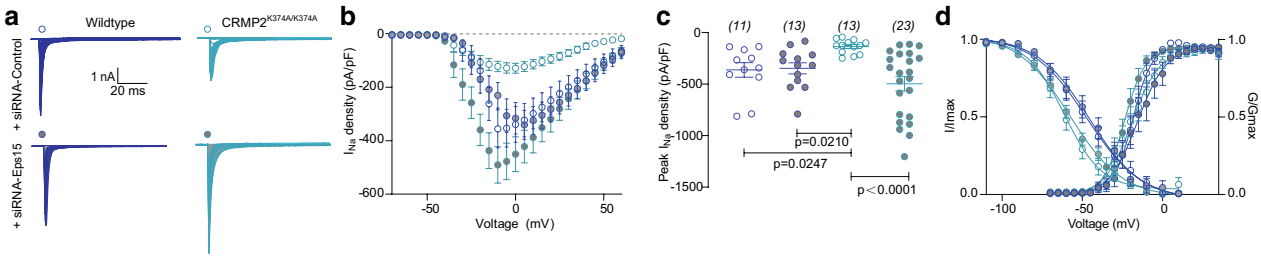

Fig. 5 CRMP2-mediated decrease in sodium currents observed in DRGs from CRMP2$^{K374A/K374A}$ mice is rescued in cells lacking Eps15. **a** Representative sodium current traces recorded from small-sized DRG neurons of WT and CRMP2$^{K374A/K374A}$ female mice, in response to depolarization steps from − 70 to + 60 mV from a holding potential of − 60 mV. **b** Summary of current density–voltage curves and **c** peak current density (pA/pF) from DRG neurons. Total sodium current density was significantly smaller in DRGs from homozygous female mice vs. DRG neurons from WT + siRNA-Control (n = 13 and 11 cells/condition, p = 0.0247, Kruskal–Wallis test with Dunn's post hoc), vs. DRG neurons from WT + siRNA-Eps15 (n = 13 and 13, p = 0.0210, Kruskal–Wallis test with Dunn's post hoc), and vs. DRG neurons from CRMP2$^{K374A/K374A}$ + siRNA-Eps15 (n = 13 and 23, p < 0.0001, Kruskal–Wallis test with Dunn's post hoc). **d** Boltzmann fits for normalized conductance *G/Gmax*-voltage relations for voltage dependent activation and inactivation of the sensory neurons. Half-maximal activation and inactivation ($V_{1/2}$) and slope values (*k*) for activation and inactivation are presented in Table 1. There were no significant differences in $V_{1/2}$ and *k* values of activation and inactivation between genotype and treatment (One-way ANOVA with Dunnett's post hoc test). Error bars indicate mean ± SEM

[24, 25]. We have demonstrated that this CRMP2-regulation is selective for $Na_V1.7$. In our previous study [37], we reported that in both male and female CRMP2$^{K374A/K374A}$ mice, calcium and potassium channels were not affected. Likewise, $Na_V1.1$, $Na_V1.2$, $Na_V1.3$, $Na_V1.5$, $Na_V1.6$, $Na_V1.8$, and $Na_V1.9$ channels were not regulated when CRMP2 SUMOylation was lost in a heterologous expression system, and in rat and human DRGs [25], ruling out the possibility that other channels are compromised by loss of CRMP2 SUMOylation. In chronic neuropathic pain, we found that enhanced $Na_V1.7$ functional expression correlates with an increase of CRMP2 SUMOylation [25, 39]. Interestingly, expressing a SUMO-null CRMP2 mutant (K374A) in rats with neuropathic pain was sufficient to reverse mechanical allodynia [9]. Also, CRMP2$^{K374A/K374A}$ male and female mice are resistant to the development of mechanical allodynia after SNI [19] (Figs. 1 and 6). In male CRMP2$^{K374A/K374A}$ mutant, $Na_V1.7$ currents are not compromised as in females [37]; however, after SNI, $Na_V1.7$ channels are expected to be involved in males due to an increase in CRMP2 SUMOylation [26]. Because $Na_V1.7$ endocytosis is clathrin-dependent [25], we reasoned that inhibiting clathrin assembly with Pitstop2 in vivo may restore mechanical allodynia in male mice. We show that this resistance of CRMP2$^{K374A/K374A}$ mice is dependent on

Table 1 Effects of silencing Numb, Nedd4-2 and Eps15 on gating properties of sodium channels in DRG neurons from WT and CRMP2$^{K374A/K374A}$ female mice

	WT		CRMP2$^{K374A/K374A}$	
	siRNA			
	Control	*Numb*	*Control*	*Numb*
Activation				
$V_{1/2}$	− 13.2±0.5 (15)	− 17.9 ± 0.7 (11)	− 17.8 ± 1.2 (9)	17.5 ± 0.9 (15)
k	5.6 ± 0.4 (15)	6.0 ± 0.6 (11)	8.6 ± 1.1 (9)	7.6 ± 0.8 (15)
Inactivation				
$V_{1/2}$	− 47.1 ± 1.4 (13)	− 56.8 ± 1.2 (12)	− 56.2 ± 1.7 (10)	− 47.8 ± 2.4 (15)
k	− 12.3 ± 1.4 (13)	− 10.5 ± 1.1 (12)	− 14.8 ± 1.7 (10)	− 17.9 ± 2.6 (15)
	Control	*Nedd4-2*	*Control*	*Nedd4-2*
Activation				
$V_{1/2}$	− 18.5 ± 0.7 (12)	− 17.3 ± 1.0 (15)	− 19.2 ± 1.0 (12)	− 19.4 ± 0.7 (19)
k	5.9 ± 0.6 (12)	8.2 ± 0.9 (15)	8.5 ± 1 (12)	5.8 ± 0.6 (19)
Inactivation				
$V_{1/2}$	− 47.3 ± 2.5 (11)	− 47.5 ± 2.5 (15)	− 61.2 ± 1.7 (13)	− 52.0 ± 2.0 (20)
k	− 17.0 ± 2.7 (11)	− 18.7 ± 2.8 (15)	− 11.7 ± 1.6 (13)	− 18.2 ± 2.2 (20)
	Control	*Eps15*	*Control*	*Eps15*
Activation				
$V_{1/2}$	− 18.5 ± 0.7 (12)	− 15.6 ± 1.3 (13)	− 19.2 ± 1.0 (12)	− 23.8 ± 0.7 (17)
k	5.9 ± 0.6 (12)	9.0 ± 1.2 (13)	8.5 ± 1.0 (12)	6.6 ± 0.6 (17)
Inactivation				
$V_{1/2}$	− 47.3 ± 2.5 (11)	− 45.7 ± 2.4 (11)	− 61.2 ± 1.7 (13)	− 57.8 ± 1.6 (23)
k	− 17.0 ± 2.7 (11)	− 16.4 ± 2.6 (11)	− 11.7 ± 1.6 (13)	− 16.4 ± 1.6 (23)

Values are means ± SEM calculated from fits of the data from the indicated number of individual cells (in parentheses) to the Boltzmann equation; $V_{1/2}$ midpoint potential (mV) for voltage-dependent activation or inactivation; *k*, slope factor. These values pertain to Figs. 3, 4 and 5. Data were analyzed with one-way ANOVA with Dunnett's post hoc test. No statistically significant differences are reported

clathrin-mediated endocytosis (Figs. 1 and 6). In other words, Pitstop2 contributes to the re-establishment of mechanical allodynia in these mice probably by maintaining $Na_V1.7$ membrane expression where it is available for voltage-dependent activation. This finding correlates with our previous reports that Pitstop2 prevents Na^+ current density reductions imposed by loss of CRMP2 SUMOylation [25, 37] (Fig. 6b). Therefore, our data suggests that the association of non-SUMOylated CRMP2 with the clathrin machinery contributes to mitigate pain. This in accordance with our observations that interfering with SUMOylation of CRMP2, promotes clathrin-mediated endocytosis of $Na_V1.7$ [25] and reverses mechanical allodynia [39].

Loss of CRMP2 SUMOylation increases its association with Numb, Nedd4-2 and Eps15. Although there is no information regarding the direct role of CRMP2 in recycling, when CRMP2 is not SUMOylated, $Na_V1.7$ channels colocalize with Rab11-positive recycling endosomes [25]. Numb is involved in clathrin-dependent endocytosis at the plasma membrane; it associates with the appendage domain of α adaptin, a subunit of the clathrin adaptor complex AP2, a major component of clathrin-coated pits [32]. Numb can interact in vivo and in vitro with Eps15, a component of the endocytic machinery [40], that also interacts with AP2 [41]. The E3 ubiquitin ligase Nedd4-2 is a potent post translational regulator of $Na_V1.7$ and NaV1.8 voltage-gated sodium channels [33]. Its down-regulation leads to hyperexcitability of DRG neurons and contributes to the onset of chronic neuropathic pain [33]. We recently reported that ~ 76% of the sodium current is contributed by $Na_V1.7$ sodium channels in DRGs from WT and CRMP2$^{K374A/K374A}$ female mice [37]. This fraction was determined by applying PF05089771, a $Na_V1.7$-specific blocker [42]. In their male counterparts, $Na_V1.7$ sodium currents represented 53% and 58% of total sodium currents from WT and CRMP2$^{K374A/K374A}$ DRGs, respectively [37]. To assess if this difference between males and females could be due to differences in the expression of the proteins that regulate $Na_V1.7$ endocytosis, we performed western blot analyses. In naïve wildtype mice, the protein levels of Numb, Nedd4-2 and Eps15 in the lumbar DRG are similar between males and females (Fig. 2 and 6b). Alternatively, a sex-dependent difference in the expression of endocytic proteins may develop after nerve injury. Nedd4-2 expression

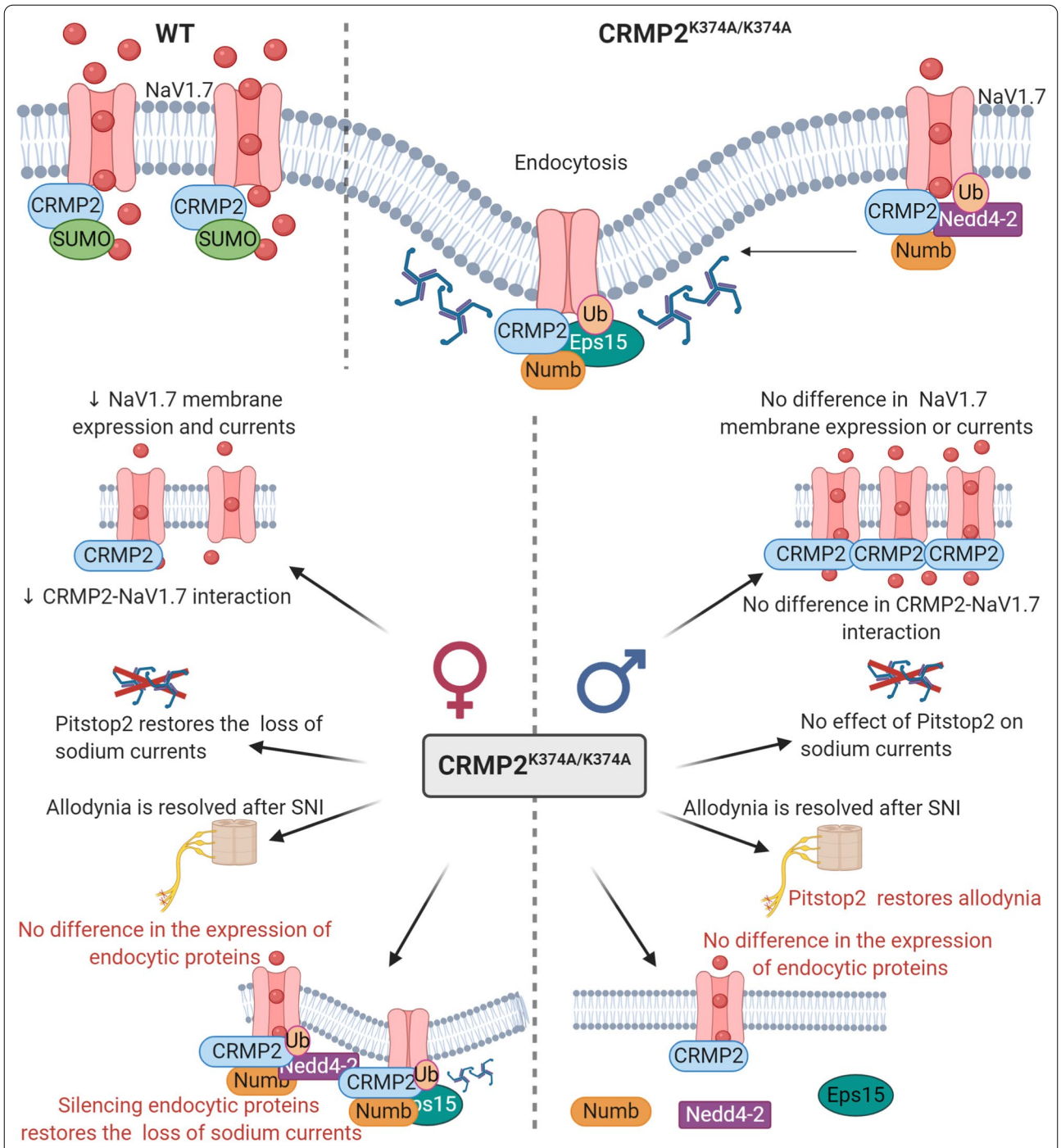

Fig. 6 Schematic representation of CRMP2 regulation of $Na_V1.7$ channels. Top: In wildtype (WT) mice (left), when CRMP2 is SUMOylated it interacts with $Na_V1.7$ channels to enhance their trafficking to the plasma membrane. In $CRMP2^{K374A/K374A}$ mice (right), non-SUMOylated CRMP2 recruits Numb, Nedd4-2 and Eps15 to trigger clathrin-mediated endocytosis of $Na_V1.7$ channels. Bottom: Sex specific differences of female (left) and male (right) $CRMP2^{K374A/K374A}$ mice compared to their WT littermates. In female mice: (i) $Na_V1.7$ membrane expression, currents, and CRMP2-$Na_V1.7$ interaction are reduced [37], (ii) Pitstop2 restores the loss of sodium currents and allodynia [37], (iii) in basal conditions no difference in the expression of endocytic proteins is seen and, (iv) silencing Numb, Nedd4-2 and Eps15 restores the loss of sodium currents. In male mice: (i) $Na_V1.7$ membrane expression, currents, and CRMP2-$Na_V1.7$ interaction are not modified [37], (ii) Pitstop2 has no effect on sodium currents (37) but restores mechanical allodynia, and (iii) in basal conditions no difference in the expression of Numb, Nedd4-2 and Eps15 is observed. Red text represents the data obtained in this study

was reported to be decreased in sciatic nerve after SNI [33]. We also found that CRMP2 SUMOylation [26] and phosphorylation by Cdk5 [27, 28] were upregulated in DRG and spinal cord following SNI. These modifications decrease the interaction of CRMP2 with the endocytic proteins Numb, Nedd4-2 and Eps15 [25]. Therefore, independent of the expression level of these endocytic proteins in SNI, the dysregulation of CRMP2 post-translational modifications prevents their recruitment to $Na_V1.7$ [31]. This could explain why the $CRMP2^{K374A/K374A}$ genotype renders both male and female mice resistant to SNI [37]. These data leave open the possibility (not tested here) that in females there is a lesser degree of interaction between CRMP2 and these endocytic proteins in the DRG, compared to males. In support of this possibility, we found that CRMP2 interaction with $Na_V1.7$ was marginal in wildtype males compared to females [37].

$CRMP2^{K374A/K374A}$ mutation decreases sodium currents in a sex-specific manner [37]. Total sodium currents are decreased (~40%) in female $CRMP2^{K374A/K374A}$ DRG but not in males [19] (Fig. 6b). For this reason, we decided to determine the functional relevance of these endocytic proteins in our female knock-in mice. Recordings of total sodium currents revealed that the decreased current density, ranging from 50 to ~63.7%, was prevented when Numb, Nedd4-2 and Eps15 were individually silenced in acutely dissociated DRG neurons (Figs. 3, 4 and 5). By knocking down each of these proteins individually in sensory neurons, we showed that they coordinate $Na_V1.7$ internalization when CRMP2 SUMOylation is lost. These results correlate with our finding that following specific reduction of these CRMP2-interacting proteins, the inhibition of $Na_V1.7$ currents by loss of CRMP2 SUMOylation is rescued [25].

A limitation of our study is that we cannot strictly rule out the possibility that reversal of allodynia by blocking clathrin mediated endocytosis occurs solely due to CRMP2. Preventing clathrin mediated endocytosis with Pitstop2 resulted in restoration of pain hypersensitivity in $CRMP2^{K374A/K374A}$ mice which we conclude is because of this small molecule's effect on antagonism of $Na_V1.7$ endocytosis that is otherwise facilitated by the CRMP2 SUMO-null mutation. However, the effect of Pitstop2 might occur via many other pathways, as proteins other than $Na_V1.7$ are also endocytosed. Preventing clathrin mediated endocytosis with Pitstop2 failed to elicit a change in SNI-induced pain hypersensitivity in WT littermates, leading us to conclude that the mutation in CRMP2 is the reason underscoring this difference. However, a caveat here is that in WT mice the withdrawal thresholds following SNI are already so low that any putative further effect of Pitstop2 would be undetectable, thus making it difficult to rule out the contribution of events completely unrelated to CRMP2. But when injected intrathecally 36 h after intraplantar injection of complete Freund's adjuvant (CFA), which causes sustained inflammatory pain, inhibitors of dynamin and clathrin were still able to reverse preexisting mechanical hyperalgesia in wildtype mice [43], arguing against this assertion.

In summary, in WT mice, SUMOylation of CRMP2 allows for CRMP2-$Na_V1.7$ interaction and $Na_V1.7$ channel peregrination to the plasma membrane. In $CRMP2^{K374A/K374A}$ mice, non-SUMOylated CRMP2 triggers $Na_V1.7$ endocytosis by recruiting Numb, Nedd4-2 which ubiquitinates $Na_v1.7$ [33] and Eps15 which induces membrane curvature [35] (Fig. 6). However, while the above mechanism is true in female, but not male, DRG neurons from naïve mice, we found that in neuropathic pain conditions, pain assessment in male and female animals is indistinguishable [37] (Fig. 1). Comparing female $CRMP2^{K374A/K374A}$ with WT mice, we note: (i) $Na_V1.7$ membrane expression, currents, and CRMP2-$Na_V1.7$ interaction are decreased, (ii) Pitstop2 restores the loss of sodium currents and mechanical allodynia, (iii) no difference in the expression of endocytic proteins is observed in basal conditions, and (iv) silencing these endocytic proteins restores the loss of sodium currents. This granularity in regulation of $Na_V1.7$ membrane expression, a 'coding' of the function of the channel, may be utilized to design new therapeutics for chronic pain. In support of this, we used a CRMP2 SUMOylation blocking peptide strategy as a proof of concept to demonstrate that preventing this modification can reverse established chronic allodynia in neuropathic pain [44]. This unique approach will allow for the inhibition of enhanced $Na_V1.7$ function reported in neuropathic pain while leaving intact the pool of the channels participating in physiological pain sensation.

Materials and methods

Animals

All animal use was conducted in accordance with the National Institutes of Health guidelines, and the study was carried out in strict accordance with recommendations in the Guide for the Care and Use of Laboratory Animals of the University of Arizona (Protocol #: 16-141). Wildtype littermate and $CRMP2^{K374A/K374A}$ mice were housed and bred in the University of Arizona Laboratory Animal Research Center. Mice were housed in groups of 4–5 in a dedicated housing facility with ad libitum access to food and water on a 12-h light/dark cycle.

Antibodies and siRNAs

Biochemical analysis of protein content by Western blot used the following antibodies: Numb (cat. no. ab4147;

Abcam), Eps15 (cat. no. ab174291; Abcam), Nedd4-2 (cat. no. ab131167 RRID: AB_11157800; Abcam), and βIII-Tubulin (cat. no. G712A; Promega). For RNA interference, siRNA Numb (5′-TAACTGGGAAGCTACACT TTCCAGT-3′), siRNA Nedd4-2 (5′-CATACTATGTCA ATCATAATT-3′), siRNA Eps15 (5′-CCCAGGCAATGA TAGTCCCAAAGAA-3′), and siRNA control (cat. no. 12935300) were obtained from Thermo Fisher Scientific.

Western blot preparation and analysis.

Indicated samples were loaded on 4–20% Novex gels (cat. no. EC60285BOX; Thermo Fisher Scientific). Proteins were transferred for 1 h at 120 V using TGS [25 mM Tris, pH 8.5,192 mM glycine, 0.1% (mass/vol) SDS], 20% (vol/vol) methanol as transfer buffer to PVDF membranes (0.45 μm; cat. no. IPVH00010; Millipore), preactivated in pure methanol. After transfer, the membranes were blocked at room temperature for 1 h with TBST (50 mM Tris·HCl, pH 7.4, 150 mM NaCl, 0.1% Tween 20) with 5% (mass/vol) nonfat dry milk, and then incubated separately in indicated primary antibodies in TBST, 5% (mass/vol) BSA, overnight at 4 °C. Following incubation in HRP-conjugated secondary antibodies from Jackson Immuno Research, blots were revealed by enhanced luminescence (WBKLS0500; Millipore) before exposure to photographic film. Films were scanned, digitized, and quantified by using Un-Scan-It gel scanning software (version 7.1; Silk Scientific) (Additional file 2: Figure S1).

Preparation of acutely dissociated dorsal root ganglia neurons from wildtype (WT) and CRMP2$^{K374A/K374A}$ mice

Wildtype and CRMP2$^{K374A/K374A}$ mice were deeply anaesthetized with isoflurane overdose (5% in oxygen) and sacrificed by decapitation. Dorsal root ganglia (DRG) were quickly removed, trimmed at their roots, and enzymatically digested in 3 mL bicarbonate-free, serum-free, sterile DMEM (Cat# 11,965, Thermo Fisher Scientific, Waltham, MA) solution containing neutral protease (1.87 mg/ml, Cat#LS02104; Worthington, Lakewood, NJ) and collagenase type I (3 mg/mL, Cat# LS004194, Worthington, Lakewood, NJ) and incubated for 50 min at 37 °C under gentle agitation. Dissociated DRG neurons were then gently centrifuged to collect cells and washed with DRG media (DMEM containing 1% penicillin/streptomycin sulfate from 10,000 μg/mL stock, and 10% fetal bovine serum (Hyclone). Collected cells were resuspended in Nucleofector transfection reagent containing siRNA at a working concentration of 600 nM. Then, cells were subjected to electroporation protocol O-003 in an Amaxa Biosystem (Lonza) and plated onto 12-mm poly-D-lysine- and laminin-coated glass coverslips. Transfection efficiencies were routinely between 20 and 30%, with approximately ~10% cell death. siRNA transfection was verified by GFP fluorescence.

Whole-cell electrophysiological recordings of sodium currents in acutely dissociated DRG neurons from WT and CRMP2$^{K374A/K374A}$ mice

All recordings were obtained from acutely dissociated DRG neurons from WT and CRMP2$^{K374A/K374A}$ mice using procedures as described previously [37]. Whole-cell voltage-clamp recordings were performed between 48 and 72 h after transfection at room temperature, using an EPC 10 Amplifier-HEKA. The external solution consisted of (in mM): 140 NaCl, 30 tetraethylammonium chloride, 10 D-glucose, 3 KCl, 1 $CaCl_2$, 0.5 $CdCl_2$, 1 $MgCl_2$, and 10 HEPES (pH 7.3, mOsm/L = 310–315) and internal solution contained the following (in mM): 140 CsF, 10 NaCl, 1.1 Cs-EGTA, and 15 HEPES (pH 7.3, mOsm/L = 290–310). DRG neurons were subjected to current–voltage (I–V) and activation/inactivation voltage protocols as follows: (a) I–V protocol: from a − 60 mV holding potential, cells were depolarized in 150-ms voltage steps from − 70 to + 60 mV (5-mV increments) which allowed acquisition of current density values such that we could analyze activation of sodium channels as a function of current vs voltage and infer peak current density (normalized to cell capacitance (in picofarads, pF)), which occurred between ~ 0 and 10 mV; (b) inactivation protocol: from a holding potential of − 60 mV, cells were subjected to hyperpolarizing/repolarizing pulses for 1 s between − 120 and 10 mV (+ 10 mV steps). Pipettes were pulled from standard wall borosilicate glass capillaries (Warner Instruments) with a horizontal puller (Model P-97, Sutter Instruments) and heat-polished to final resistances of 1–4 MΩ when filled with internal solutions. Capacitive artifacts were fully compensated, and series resistance was compensated by ~ 70%. Recordings made from cells with greater than a 20% shift in series resistance compensation error were excluded from analysis. This error was not corrected in the analysis of activation and inactivation. Linear leak currents were digitally subtracted through P/4 method for voltage clamp experiments. Signals were filtered at 10 kHz and digitized at 10–20 kHz. Analysis was performed by using Fitmaster software (HEKA) and Origin 9.0 software (OriginLab).

Spared nerve injury (SNI) model of neuropathic pain and assessment of mechanical allodynia

For the spared nerve injury (SNI) model, we transected the common peroneal and tibial branches of the right sciatic nerve with ~1 mm of nerve removed and left the sural nerve intact. Age-matched and genotyped WT and CRMP2$^{K374A/K374A}$ mice were habituated in plastic chambers on a mesh floor. Calibrated von Frey

filaments with sequentially increasing spring coefficients were applied to the hind paw of each mouse, which allowed for the consistent application of constant force stimuli. The test was performed on the lateral part of the right plantar surface where the sural nerve innervates the hind paw. One filament was applied five times in a round of testing. The filament force evoking paw withdrawal more than three times in a round of testing was defined as the mechanical threshold. The cutoff threshold was 4 g.

Statistical analyses

All data was first tested for a Gaussian distribution using a D'Agostino-Pearson test (Prism 8 Software, Graphpad, San Diego, CA). The statistical significance of differences between means was determined by a parametric ANOVA followed by Dunnett's post hoc or a non-parametric Kruskal Wallis test followed by Dunn's post-hoc test depending on if datasets achieved normality. Behavioral data with a time course were analyzed by Two-way ANOVA with Sidak's post hoc test. Differences were considered significant if $p \leq 0.05$. Error bars in the graphs represent mean ± SEM. All data were plotted in Prism 8.

Supplementary Information

The online version contains supplementary material available at https://doi.org/10.1186/s13041-020-00714-1.

Additional file 1: Table S1. Raw quantified numerical data for all figures in the manuscript.

Additional file 2: Figure S1. Raw immunoblot of Numb, Nedd4-2 and Eps15 expression in male and female mice DRGs. Raw Western blots showing the expression of the endocytic proteins Numb, Nedd4-2 and Eps15 in lumbar DRG from male and female wildtype mice. βIII-tubulin served as a loading control.

Abbreviations

Cdk5: Cyclin-dependent kinase 5; CRMP2: Collapsin response mediator protein 2; DRG: Dorsal root ganglia; Eps15: Epidermal growth factor receptor pathway substrate 15; *k*: Slope factor; $Na_V1.7$: Voltage-gated sodium channel family 1.7; Nedd4-2: Neuronal precursor cell expressed developmentally downregulated-4 type 2.; SNI: Spinal nerve injury; TTX-S: Tetrodotoxin-sensitive; *V1/2*: Midpoint potentials.

Authors' contributions

R.K. and A.M. developed the concept and designed experiments; A.M., K.G., and D.R., collected and analyzed data; C.L.M. performed animal behavior studies; R.K. provided funding; D.R., K.G., R.K. and A.M. wrote the manuscript; and R.K. and A.M. supervised all aspects of this project. All authors had the opportunity to discuss results and comment on the manuscript. All authors read and approved the final manuscript.

Funding

This work is supported by National Institutes of Health awards to R.K. (NINDS (NS098772 and NS120663), NIDA (DA042852).

Availability of data and materials

Full blots of the partial immunoblots shown in Fig. 2 of manuscript are presented in Additional file 2: Figure S1. All quantified numerical data is presented in Additional file 1: Table S1.

Ethics approval and consent to participate

Not applicable.

Ethics approval for use of animals

The University of Arizona's College of Medicine Institutional Animal Care and Use Committee (IACUC) sanctioned all experiments.

Consent for publication

Not applicable.

Competing interests

R. Khanna is the co-founder of Regulonix LLC, a company developing non-opioids drugs for chronic pain. In addition, R. Khanna has patents US10287334 and US10441586 issued to Regulonix LLC. R. The other authors declare no competing financial interest.

Author details

[1] Department of Pharmacology, College of Medicine, University of Arizona, 1501 North Campbell Drive, P.O. Box 245050, Tucson, AZ 85724, USA. [2] Comprehensive Pain and Addiction Center, The University of Arizona, Tucson, AZ 85724, USA.

Received: 30 September 2020 Accepted: 7 December 2020
Published online: 21 January 2021

References

1. Black JA, Frezel N, Dib-Hajj SD, Waxman SG. Expression of Nav1.7 in DRG neurons extends from peripheral terminals in the skin to central preterminal branches and terminals in the dorsal horn. Mol Pain. 2012;8:82.
2. Klugbauer N, Lacinova L, Flockerzi V, Hofmann F. Structure and functional expression of a new member of the tetrodotoxin-sensitive voltage-activated sodium channel family from human neuroendocrine cells. EMBO J. 1995;14(6):1084–90.
3. Rush AM, Cummins TR, Waxman SG. Multiple sodium channels and their roles in electrogenesis within dorsal root ganglion neurons. J Physiol. 2007;579(Pt 1):1–14.
4. Dib-Hajj SD, Cummins TR, Black JA, Waxman SG. Sodium channels in normal and pathological pain. Annu Rev Neurosci. 2010;33:325–47.
5. Drenth JP, Waxman SG. Mutations in sodium-channel gene SCN9A cause a spectrum of human genetic pain disorders. J Clin Investig. 2007;117(12):3603–9.
6. Hameed S. Nav1.7 and Nav1.8: Role in the pathophysiology of pain. Mol Pain. 2019;15:1744806919858801.
7. Moutal A, Francois-Moutal L, Brittain JM, Khanna M, Khanna R. Differential neuroprotective potential of CRMP2 peptide aptamers conjugated to cationic, hydrophobic, and amphipathic cell penetrating peptides. Front Cell Neurosci. 2014;8:471.
8. Brittain JM, Pan R, You H, Brustovetsky T, Brustovetsky N, Zamponi GW, et al. Disruption of NMDAR-CRMP-2 signaling protects against focal cerebral ischemic damage in the rat middle cerebral artery occlusion model. Channels (Austin). 2012;6(1):52–9.
9. Brittain JM, Chen L, Wilson SM, Brustovetsky T, Gao X, Ashpole NM, et al. Neuroprotection against traumatic brain injury by a peptide derived from the collapsin response mediator protein 2 (CRMP2). J Biol Chem. 2011;286(43):37778–92.
10. Brittain MK, Brustovetsky T, Sheets PL, Brittain JM, Khanna R, Cummins TR, et al. Delayed calcium dysregulation in neurons requires both the NMDA receptor and the reverse Na+/Ca2+ exchanger. Neurobiol Dis. 2012;46(1):109–17.
11. Brustovetsky T, Pellman JJ, Yang XF, Khanna R, Brustovetsky N. Collapsin response mediator protein 2 (CRMP2) interacts with N-methyl-D-aspartate (NMDA) receptor and Na+/Ca2+ exchanger and regulates their functional activity. J Biol Chem. 2014;289(11):7470–82.

12. Brittain JM, Duarte DB, Wilson SM, Zhu W, Ballard C, Johnson PL, et al. Suppression of inflammatory and neuropathic pain by uncoupling CRMP-2 from the presynaptic Ca(2)(+) channel complex. Nat Med. 2011;17(7):822–9.
13. Brittain JM, Piekarz AD, Wang Y, Kondo T, Cummins TR, Khanna R. An atypical role for collapsin response mediator protein 2 (CRMP-2) in neurotransmitter release via interaction with presynaptic voltage-gated calcium channels. J Biol Chem. 2009;284(45):31375–90.
14. Brittain JM, Wang Y, Eruvwetere O, Khanna R. Cdk5-mediated phosphorylation of CRMP-2 enhances its interaction with CaV2.2. FEBS Lett. 2012;586(21):3813–8.
15. Francois-Moutal L, Wang Y, Moutal A, Cottier KE, Melemedjian OK, Yang X, et al. A membrane-delimited N-myristoylated CRMP2 peptide aptamer inhibits CaV2.2 trafficking and reverses inflammatory and postoperative pain behaviors. Pain. 2015;156(7):1247–64.
16. Moutal A, Wang Y, Yang X, Ji Y, Luo S, Dorame A, et al. Dissecting the role of the CRMP2-neurofibromin complex on pain behaviors. Pain. 2017;158(11):2203–21.
17. Piekarz AD, Due MR, Khanna M, Wang B, Ripsch MS, Wang R, et al. CRMP-2 peptide mediated decrease of high and low voltage-activated calcium channels, attenuation of nociceptor excitability, and anti-nociception in a model of AIDS therapy-induced painful peripheral neuropathy. Mol Pain. 2012;8(1):54.
18. Wang Y, Brittain JM, Wilson SM, Khanna R. Emerging roles of collapsin response mediator proteins (CRMPs) as regulators of voltage-gated calcium channels and synaptic transmission. Commun Integr Biol. 2010;3(2):1–4.
19. Xie JY, Chew LA, Yang X, Wang Y, Qu C, Wang Y, et al. Sustained relief of ongoing experimental neuropathic pain by a CRMP2 peptide aptamer with low abuse potential. Pain. 2016;157(9):2124–40.
20. Chew LA, Bellampalli SS, Dustrude ET, Khanna R. Mining the Nav1.7 interactome: Opportunities for chronic pain therapeutics. Biochem Pharmacol. 2019;163:9–20.
21. Chew LA, Khanna R. CRMP2 and voltage-gated ion channels: potential roles in neuropathic pain. Neuronal Signal. 2018. https://doi.org/10.1042/NS20170220.
22. Stratton H, Boinon L, Moutal A, Khanna R. Coordinating synaptic signaling with CRMP2. Int J Biochem Cell Biol. 2020;124:105759.
23. Khanna R, Moutal A, Perez-Miller S, Chefdeville A, Boinon L, Patek M. Druggability of CRMP2 for neurodegenerative diseases. ACS Chem Neurosci. 2020;11(17):2492–505.
24. Dustrude ET, Wilson SM, Ju W, Xiao Y, Khanna R. CRMP2 protein SUMOylation modulates NaV1.7 channel trafficking. J Biol Chem. 2013;288(34):24316–31.
25. Dustrude ET, Moutal A, Yang X, Wang Y, Khanna M, Khanna R. Hierarchical CRMP2 posttranslational modifications control NaV1.7 function. Proc Natl Acad Sci USA. 2016;113(52):E8443–52.
26. Moutal A, Dustrude ET, Largent-Milnes TM, Vanderah TW, Khanna M, Khanna R. Blocking CRMP2 SUMOylation reverses neuropathic pain. Mol Psychiatry. 2018;23(11):2119–21.
27. Moutal A, Luo S, Largent-Milnes TM, Vanderah TW, Khanna R. Cdk5-mediated CRMP2 phosphorylation is necessary and sufficient for peripheral neuropathic pain. Neurobiol Pain. 2019;5.
28. Yu J, Moutal A, Dorame A, Bellampalli SS, Chefdeville A, Kanazawa I, et al. Phosphorylated CRMP2 regulates spinal nociceptive neurotransmission. Mol Neurobiol. 2019;56(7):5241–55.
29. Gomez K, Vallecillo TGM, Moutal A, Perez-Miller S, Delgado-Lezama R, Felix R, et al. The role of cyclin-dependent kinase 5 in neuropathic pain. Pain. 2020;161(12):2674–89.
30. Moutal A, Ji Y, Bellampalli SS, Khanna R. Differential expression of Cdk5-phosphorylated CRMP2 following a spared nerve injury. Mol Brain. 2020;13(1):97.
31. Moutal A, White KA, Chefdeville A, Laufmann RN, Vitiello PF, Feinstein D, et al. Dysregulation of CRMP2 post-translational modifications drive its pathological functions. Mol Neurobiol. 2019;56(10):6736–55.
32. Santolini E, Puri C, Salcini AE, Gagliani MC, Pelicci PG, Tacchetti C, et al. Numb is an endocytic protein. J Cell Biol. 2000;151(6):1345–52.
33. Laedermann CJ, Cachemaille M, Kirschmann G, Pertin M, Gosselin RD, Chang I, et al. Dysregulation of voltage-gated sodium channels by ubiquitin ligase NEDD4-2 in neuropathic pain. J Clin Investig. 2013;123(7):3002–13.
34. Woelk T, Oldrini B, Maspero E, Confalonieri S, Cavallaro E, Di Fiore PP, et al. Molecular mechanisms of coupled monoubiquitination. Nat Cell Biol. 2006;8(11):1246–54.
35. Horvath CA, Vanden Broeck D, Boulet GA, Bogers J, De Wolf MJ. Epsin: inducing membrane curvature. Int J Biochem Cell Biol. 2007;39(10):1765–70.
36. Dustrude ET, Perez-Miller S, Francois-Moutal L, Moutal A, Khanna M, Khanna R. A single structurally conserved SUMOylation site in CRMP2 controls NaV1.7 function. Channels (Austin). 2017;11(4):316–28.
37. Moutal A, Cai S, Yu J, Stratton HJ, Chefdeville A, Gomez K, et al. Studies on CRMP2 SUMOylation-deficient transgenic mice identify sex-specific Nav1.7 regulation in the pathogenesis of chronic neuropathic pain. Pain. 2020;161(11):2629–51.
38. von Kleist L, Stahlschmidt W, Bulut H, Gromova K, Puchkov D, Robertson MJ, et al. Role of the clathrin terminal domain in regulating coated pit dynamics revealed by small molecule inhibition. Cell. 2011;146(3):471–84.
39. Moutal A, Li W, Wang Y, Ju W, Luo S, Cai S, et al. Homology-guided mutational analysis reveals the functional requirements for antinociceptive specificity of collapsin response mediator protein 2-derived peptides. Br J Pharmacol. 2018;175(12):2244–60.
40. Salcini AE, Confalonieri S, Doria M, Santolini E, Tassi E, Minenkova O, et al. Binding specificity and in vivo targets of the EH domain, a novel protein-protein interaction module. Genes Dev. 1997;11(17):2239–49.
41. Benmerah A, Begue B, Dautry-Varsat A, Cerf-Bensussan N. The ear of alpha-adaptin interacts with the COOH-terminal domain of the Eps 15 protein. J Biol Chem. 1996;271(20):12111–6.
42. Alexandrou AJ, Brown AR, Chapman ML, Estacion M, Turner J, Mis MA, et al. Subtype-selective small molecule inhibitors reveal a fundamental role for Nav1.7 in nociceptor electrogenesis, axonal conduction and presynaptic release. PLoS ONE. 2016;11(4):e0152405.
43. Jensen DD, Lieu T, Halls ML, Veldhuis NA, Imlach WL, Mai QN, et al. Neurokinin 1 receptor signaling in endosomes mediates sustained nociception and is a viable therapeutic target for prolonged pain relief. Sci Transl Med. 2017;9(392):eaal3447.
44. Francois-Moutal L, Dustrude ET, Wang Y, Brustovetsky T, Dorame A, Ju W, et al. Inhibition of the Ubc9 E2 SUMO-conjugating enzyme-CRMP2 interaction decreases NaV1.7 currents and reverses experimental neuropathic pain. Pain. 2018;159(10):2115–27.

Publisher's Note

Springer Nature remains neutral with regard to jurisdictional claims in published maps and institutional affiliations.